Chapter 3
Continuous Wavelet Transform

Wavelet transform is a mathematical tool that converts a signal into a different form. This conversion has the goal to reveal the characteristics or "features" hidden within the original signal and represent the original signal more succinctly. A base wavelet is needed in order to realize the wavelet transform. The wavelet is a small wave that has an oscillating wavelike characteristic and has its energy concentrated in time. Figure 3.1 illustrates a wave (sinusoidal) and a wavelet (Daubechies 4 wavelet) (Daubechies 1992).

The difference between a wave and a wavelet is that a wave is usually smooth and regular in shape, and can be everlasting, while in contrast, a wavelet may be irregular in shape, and normally lasts only for a limited period of time. A wave (e.g., sine and cosine) is typically used as a deterministic template in the Fourier transform for representing a signal that is time-invariant or stationary. In comparison, a wavelet can serve as both a deterministic and nondeterministic template for analyzing time-varying or nonstationary signals by decomposing the signal into a 2D, time-frequency domain.

Mathematically, a wavelet is a square integrable function $\psi(t)$ that satisfies the *admissibility condition* (Chui 1992; Meyer 1993; Mallat 1998):

$$\int_{-\infty}^{\infty} \frac{|\Psi(f)|^2}{(f)} df < \infty \tag{3.1}$$

In this equation, $\Psi(f)$ is the Fourier transform (i.e., frequency domain expression) of the wavelet function $\psi(t)$ (in the time domain). The admissibility condition implies that the Fourier transform of the function $\psi(t)$ vanishes at the zero frequency; that is,

$$|\Psi(f)|^2\big|_{f=0} = 0 \tag{3.2}$$

This means that the wavelet must have a band-pass like spectrum. A zero at the zero frequency also means that the average value of the wavelet $\psi(t)$ in the time domain is zero:

$$\int_{-\infty}^{\infty} \psi(t)dt = 0 \tag{3.3}$$

R.X. Gao and R. Yan, *Wavelets: Theory and Applications for Manufacturing*,
DOI 10.1007/978-1-4419-1545-0_3,

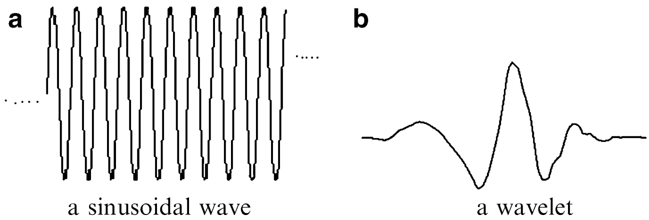

Fig. 3.1 Representation of a wave and a wavelet. (**a**) A sinusoidal wave and (**b**) a wavelet

Equation (3.3) indicates that the wavelet must be oscillatory in nature. Through the process of *dilation* (i.e., stretching or squeezing the wavelet function by $1/s$) and *translation*, (i.e., shift along time axis by τ), a family of scaled and translated wavelets can be obtained as

$$\psi_{s,\tau}(t) = \frac{1}{\sqrt{s}}\psi\left(\frac{t-\tau}{s}\right), \quad s>0,\ \tau \in R \tag{3.4}$$

The purpose of having the factor $\frac{1}{\sqrt{s}}$ in (3.4) is to ensure that the energy of the wavelet family will remain the same under different scales. For example, by assuming that the energy of the wavelet function $\psi(t)$ is given by

$$\varepsilon = \int_{-\infty}^{\infty} |\psi(t)|^2 \, dt \tag{3.5}$$

the energy of the scaled and translated wavelets $\psi_{s,\tau}(t)$ can be calculated as

$$\varepsilon' = \int_{-\infty}^{\infty} \left|\frac{1}{\sqrt{s}}\psi\left(\frac{t-\tau}{s}\right)\right|^2 dt = \frac{1}{s}\int_{-\infty}^{\infty} \left|\psi\left(\frac{t}{s}\right)\right|^2 dt = \varepsilon \tag{3.6}$$

As a result, the energy of the original base wavelet $\psi(t)$ and the scaled and translated wavelets remains the same. The relationship between $\psi(t)$ and $\psi_{s,\tau}(t)$ is illustrated in Fig. 3.2, and the process through which a signal is decomposed by analyzing it with a family of scaled and translated wavelets such as $\psi_{s,\tau}(t)$ is called the wavelet transform.

Generally, the wavelet transform can be represented in continuous (i.e., continuous wavelet transform (CWT)) as well as in discrete forms (i.e., discrete wavelet transform). The CWT of a signal $x(t)$ is defined as (Rioul and Vetterli 1991)

$$wt(s,\tau) = \frac{1}{\sqrt{s}}\int_{-\infty}^{\infty} x(t)\psi^*\left(\frac{t-\tau}{s}\right)dt \tag{3.7}$$

where $\psi^*(\cdot)$ is the complex conjugate of the scaled and shifted wavelet function $\psi(\cdot)$.

As shown in this definition, the CWT is as an integral transformation. In this sense, it is similar to the Fourier transform in that integration operation will be performed in

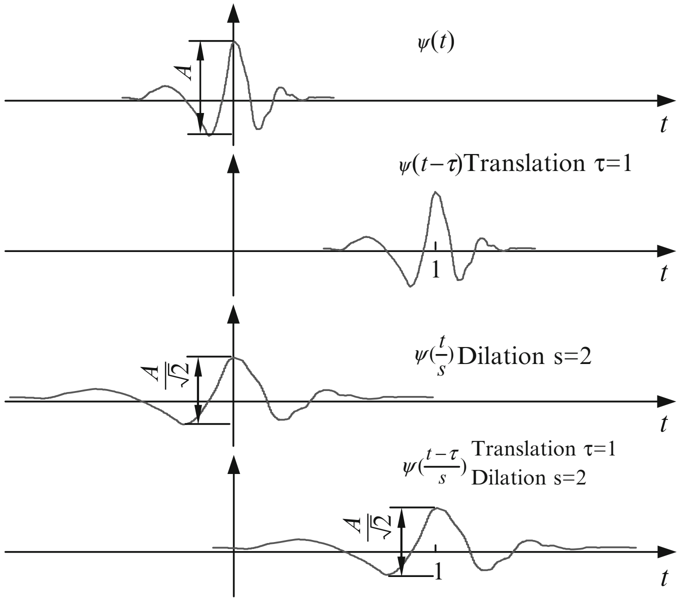

Fig. 3.2 Illustration of translation (by the time constant τ) and dilation (by the scaling factor s)

both transforms. On the other hand, as the wavelet contains two parameters (scale parameter s and translation parameter τ), transforming a signal with the wavelet basis means that such a signal will be projected into a 2D, time-scale plane, instead of the 1D frequency domain in the Fourier transform. Furthermore, because of the localization nature of the wavelet, the transformation will extract features from the signal in the time-scale plane that are not revealed in its original form, for example, what specific bearing defect-related spectral components existed at what time.

3.1 Properties of Continuous Wavelet Transform

Equation (3.7) indicates that the CWT is a linear transformation, characterized by the following properties.

3.1.1 Superposition Property

Suppose $x(t),\ y(t) \in L^2(R)$, and k_1 and k_2 are constants. If the CWT of $x(t)$ is $wt_x(s,\tau)$ and the CWT of $y(t)$ is $wt_y(s,\tau)$, then the CWT of $z(t) = k_1x(t) + k_2y(t)$ is given by

$$wt_z(s,\tau) = k_1 wt_x(s,\tau) + k_2 wt_y(s,\tau) \tag{3.8}$$

Proof: Let $wt_x(s,\tau) = \frac{1}{\sqrt{s}} \int x(t)\psi^*\left(\frac{t-\tau}{s}\right)dt$ and $wt_y(s,\tau) = \frac{1}{\sqrt{s}} \int y(t)\psi^*\left(\frac{t-\tau}{s}\right)dt$; then

$$\begin{aligned} wt_z(s,\tau) &= \frac{1}{\sqrt{s}} \int z(t)\psi^*\left(\frac{t-\tau}{s}\right)dt \\ &= \frac{1}{\sqrt{s}} \int [k_1 x(t) + k_2 y(t)]\psi^*\left(\frac{t-\tau}{s}\right)dt \\ &= k_1 \frac{1}{\sqrt{s}} \int x(t)\psi^*\left(\frac{t-\tau}{s}\right)dt + k_2 \frac{1}{\sqrt{s}} \int y(t)\psi^*\left(\frac{t-\tau}{s}\right)dt \\ &= k_1 wt_x(s,\tau) + k_2 wt_y(s,\tau) \end{aligned} \tag{3.9}$$

This proves the superposition property of the CWT.

3.1.2 Covariant Under Translation

Suppose the CWT of $x(t)$ is $wt_x(s,\tau)$; then the CWT of $x(t-t_0)$ is $wt_x(s,\tau-t_0)$. The proof of this property is shown below:

Proof: Let $x'(t) = x(t-t_0)$; then

$$wt_{x'}(s,\tau) = \frac{1}{\sqrt{s}} \int x(t-t_0)\psi^*\left(\frac{t-\tau}{s}\right)dt \tag{3.10}$$

Let $t' = t - t_0$; then

$$wt_{x'}(s,\tau) = \frac{1}{\sqrt{s}} \int x(t')\psi^*\left(\frac{t'+t_0-\tau}{s}\right)dt' = wt_x(s,\tau-t_0) \tag{3.11}$$

This means that the wavelet coefficients of $x(t-t_0)$ can be obtained by translating the wavelet coefficients of $x(t)$ along the time axis with t_0.

3.1.3 Covariant Under Dilation

Suppose the CWT of $x(t)$ is $wt_x(s,\tau)$; then the CWT of $x\left(\frac{t}{a}\right)$ is $\sqrt{a}wt_x\left(\frac{s}{a},\frac{\tau}{a}\right)$

Proof: Let $x'(t) = x\left(\frac{t}{a}\right)$; then

$$wt_{x'}(s,\tau) = \frac{1}{\sqrt{s}} \int x'(t)\psi^*\left(\frac{t-\tau}{s}\right)dt = \frac{1}{\sqrt{s}} \int x\left(\frac{t}{a}\right)\psi^*\left(\frac{t-\tau}{s}\right)dt \tag{3.12}$$

Let $t' = \frac{t}{a}$; then (3.12) becomes

$$\begin{aligned} wt_{x'}(s,\tau) &= \frac{1}{\sqrt{s}} \int x(t')\psi^*\left(\frac{at'-\tau}{s}\right) d(at') \\ &= \frac{\sqrt{a}}{\sqrt{\frac{s}{a}}} \int x(t')\psi^*\left(\frac{t'-\frac{\tau}{a}}{\frac{s}{a}}\right) dt' = \sqrt{a}wt_x\left(\frac{s}{a},\frac{\tau}{a}\right) \end{aligned} \tag{3.13}$$

Equation (3.13) indicates that, when a signal is dilated by a, its corresponding wavelet coefficients are also dilated by a along both the scale and time axes.

3.1.4 Moyal Principle

Suppose $x(t)$, $y(t) \in L^2(R)$. If the CWT of $x(t)$ is $wt_x(s,\tau)$ and the CWT of $y(t)$ is $wt_y(s,\tau)$; that is,

$$wt_x(s,\tau) = \langle x(t), \psi_{s,\tau}(t)\rangle \tag{3.14a}$$

$$wt_y(s,\tau) = \langle y(t), \psi_{s,\tau}(t)\rangle \tag{3.14b}$$

then

$$\langle wt_x(s,\tau), wt_y(s,\tau)\rangle = C_\psi \langle x(t), y(t)\rangle \tag{3.15}$$

where $C_\psi = \int_0^\infty \frac{|\Psi(f)|^2}{f} df$. The proof of this property is as follows.

Proof According to the Parseval's theorem, the inner product of two functions in time domain can be equivalently given in the frequency domain as

$$\langle x(t), y(t)\rangle = \frac{1}{2\pi} \int X(f)Y^*(f)df \tag{3.16}$$

Consequently, we have

$$wt_x(s,\tau) = \langle x(t), \psi_{s,\tau}(t)\rangle = \frac{1}{2\pi} \int X(f)\Psi^*_{s,\tau}(f)df \tag{3.17a}$$

$$wt_y(s,\tau) = \langle y(t), \psi_{s,\tau}(t)\rangle = \frac{1}{2\pi} \int Y(f)\Psi^*_{s,\tau}(f)df \tag{3.17b}$$

From (3.4), we know that $\psi_{s,\tau}(t) = \frac{1}{\sqrt{s}}\psi\left(\frac{t-\tau}{s}\right)$. Therefore,

$$\Psi_{s,\tau}(f) = \sqrt{s}\Psi(sf)e^{-j2\pi f\tau} \tag{3.18a}$$

$$\Psi^*_{s,\tau}(f) = \sqrt{s}\Psi^*(sf)e^{j2\pi f\tau} \tag{3.18b}$$

By incorporating (3.18b) into (3.17) and utilizing the following integral relation,

$$\int e^{-j2\pi(f-f')\tau}d\tau = 2\pi\delta(f-f') \tag{3.19}$$

the left side of (3.15) can be expanded as

$$\begin{aligned}\langle wt_x(s,\tau), wt_y(s,\tau)\rangle &= \frac{s}{2\pi}\iint \frac{ds}{s^2}X(f)Y^*(f)\Psi(sf)\Psi^*(sf)df \\ &= \frac{1}{2\pi}\int\left[\int\frac{|\Psi(sf)|^2}{s}ds\right]X(f)Y^*(f)df\end{aligned} \tag{3.20}$$

As $\int\frac{|\Psi(sf)|^2}{s}ds = \int\frac{|\Psi(sf)|^2}{sf}d(sf) = \int\frac{|\Psi(f')|^2}{f'}d(f') = C_\psi$, (3.20) can be expressed as

$$\langle wt_x(s,\tau), wt_y(s,\tau)\rangle = C_\psi\frac{1}{2\pi}\int X(f)Y^*(f)df = C_\psi\langle x(t), y(t)\rangle \tag{3.21}$$

This proves the existence of Moyal principle for CWT. It is noted that C_ψ is actually the *admissibility condition* of the wavelet. Only when this condition is satisfied can the Moyal principle exist. Furthermore, if $x(t) = y(t)$, then (3.15) becomes

$$\int_0^\infty\frac{ds}{s^2}\int_{-\infty}^\infty\left|wt_x(s,\tau)^2\right|d\tau = C_\psi\int_{-\infty}^\infty|x(t)|^2dt \tag{3.22}$$

This means that the integral of the square of wavelet coefficients is proportional to the energy of the signal.

3.2 Inverse Continuous Wavelet Transform

A transformation is considered to be meaningful in practice only when its corresponding inverse transformation exists. The same principle applies to the CWT. It can be shown that, as long as the wavelet satisfies the admission condition as defined in (3.1), the inverse CWT will exist. This means that a signal can be perfectly reconstructed from its corresponding wavelet coefficients, which can be written as

$$\begin{aligned} x(t) &= \frac{1}{C_\psi}\int_0^\infty \frac{ds}{s^2}\int_{-\infty}^{\infty} wt_x(s,\tau)\psi_{s,\tau}(t)d\tau \\ &= \frac{1}{C_\psi}\int_0^\infty \frac{ds}{s^2}\int_{-\infty}^{\infty} wt_x(s,\tau)\frac{1}{\sqrt{s}}\psi\left(\frac{t-\tau}{s}\right)d\tau \end{aligned} \tag{3.23}$$

where $C_\psi = \int_0^\infty \frac{|\Psi(f)|^2}{f}df < \infty$ is the admission condition of the wavelet $\psi(t)$.

The proof of (3.23) is shown below:

Proof Assume that $x_1(t) = x(t)$, and $x_2(t) = \delta(t-t')$. As $\langle x(t), \delta(t-t')\rangle = x(t')$,

$$C_\psi x(t') = C_\psi \langle x(t), \delta(t-t')\rangle \tag{3.24}$$

According to the Mayol principle shown in (3.15), (3.24) can be further written as

$$\begin{aligned} C_\psi x(t') &= \langle wt_x(s,\tau), wt_{\delta(t-t')}(s,\tau)\rangle \\ &= \int_0^\infty \frac{ds}{s^2}\int wt_x(s,\tau)wt^*_{\delta(t-t')}(s,\tau)d\tau \\ &= \int_0^\infty \frac{ds}{s^2}\int wt_x(s,\tau)\langle\psi_{s,\tau}(t), \delta(t-t')\rangle^* d\tau \\ &= \int_0^\infty \frac{ds}{s^2}\int wt_x(s,\tau)\langle\psi_{s,\tau}(t), \delta(t-t')\rangle d\tau \\ &= \int_0^\infty \frac{ds}{s^2}\int wt_x(s,\tau)\psi_{s,\tau}(t')d\tau \\ &= \frac{1}{\sqrt{s}}\int_0^\infty \frac{ds}{s^2}\int wt_x(s,\tau)\psi\left(\frac{t'-\tau}{s}\right)d\tau \end{aligned} \tag{3.25}$$

This illustrates that the inverse CWT exists.

3.3 Implementation of Continuous Wavelet Transform

To implement the CWT, two approaches can be taken. The first approach is to obtain the wavelet coefficients directly from (3.7). The computation procedure is as follows:

1. The wavelet is placed at the beginning of the signal, and set $s = 1$ (the original, base wavelet).
2. The wavelet function at scale “1” is multiplied by the signal, integrated over all times, and then multiplied by $1/\sqrt{s}$.
3. Shift the wavelet to $t = \tau$, and get the transform value at $t = \tau$ and $s = 1$.
4. Repeat the procedure until the wavelet reaches the end of the signal.
5. Scale s is increased by a given value, and the above procedure is repeated for all s.
6. Each computation for a given s fills the single row of the time-scale plane.
7. Wavelet transform is obtained if all s are calculated.

The second approach to implementing the CWT is on the basis of the convolution theorem, which states that the Fourier transform of the convolution operation on two functions in the time domain is the product of the respective Fourier transforms of these two functions in the frequency domain (Bracewell 1999). The Fourier transform of (3.7) is expressed as

$$WT(s,f) = F\{wt(s,\tau)\} = \frac{1}{2\pi\sqrt{s}} \int_{-\infty}^{\infty} \left(\int_{-\infty}^{\infty} x(t)\psi^*\left(\frac{t-\tau}{s}\right) dt \right) e^{-j2\pi f \tau}\, d\tau \tag{3.26}$$

Applying the convolution theorem to (3.26) leads to

$$WT(s,f) = \sqrt{s}X(f)\Psi^*(sf) \tag{3.27}$$

where $X(f)$ denotes the Fourier transform of $x(t)$ and $\Psi^*(\cdot)$ denotes the Fourier transform of $\psi^*(\cdot)$. By taking the inverse Fourier transform, (3.27) is converted back into the time domain as

$$wt(s,t) = F^{-1}\{WT(s,f)\} = \sqrt{s}F^{-1}\{X(f)\Psi^*(sf)\} \tag{3.28}$$

where the symbol $F^{-1}[\cdot]$ denotes the operator of inverse Fourier transform. Therefore, the implementation of the CWT can be realized through a pair of Fourier and inverse Fourier transforms.

Figure 3.3 illustrates the procedure for implementing the CWT. After taking the Fourier transform of the signal $x(t)$ and the scaled base wavelet $\psi(s,t)$ to obtain their frequency information $X(f)$ and $\Psi(sf)$, respectively, the inner product between $X(f)$ and complex conjugate of $\Psi(sf)$ is calculated. Next, the CWT of the signal $x(t)$, denoted as $cwt(s,t)$, is obtained by taking the inverse Fourier transform on the inner product of $WT(s,f)$.

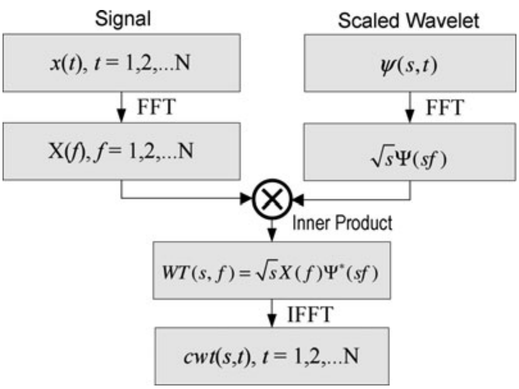

Fig. 3.3 Procedure for implementing the continuous wavelet transform

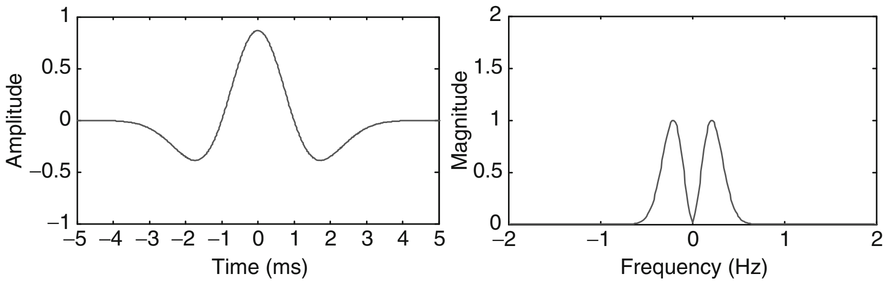

Fig. 3.4 Mexican hat wavelet (*left*) and its magnitude spectrum (*right*)

3.4 Some Commonly Used Wavelets

This section introduces several commonly used wavelets for performing the CWT.

3.4.1 *Mexican Hat Wavelets*

The Mexican hat wavelet is a normalized, second derivative of a Gaussian function, which is mathematically defined as (Mallat 1998)

$$\psi(t) = \frac{1}{\sqrt{2\pi}\sigma^3}\left(1 - \frac{\sigma^2}{t^2}\right)e^{\frac{-t^2}{2\sigma^2}} \tag{3.29}$$

Figure 3.4 illustrates the Mexican hat wavelet and its associated magnitude spectrum. The Mexican hat wavelet is often called the Ricker wavelet in geophysics, where it is frequently employed to model seismic data (Zhou and Adeli 2003; Erlebacher and Yuen 2004).

3.4.2 *Morlet Wavelet*

The Morlet wavelet is defined as (Grossmann and Morlet 1984; Teolis 1998)

$$\psi_M(t) = \frac{1}{\sqrt{\pi f_b}} e^{j2\pi f_c t}\, e^{-\frac{t^2}{f_b}} \tag{3.30}$$

where f_b is the bandwidth parameter and f_c denotes the wavelet center frequency. As an example, Fig. 3.5 illustrates the complex Morlet wavelet function and its corresponding magnitude spectrum when $f_b = 1$ Hz and $f_c = 1$ Hz. The Morlet wavelet has been widely used for identifying transient components embedded in a

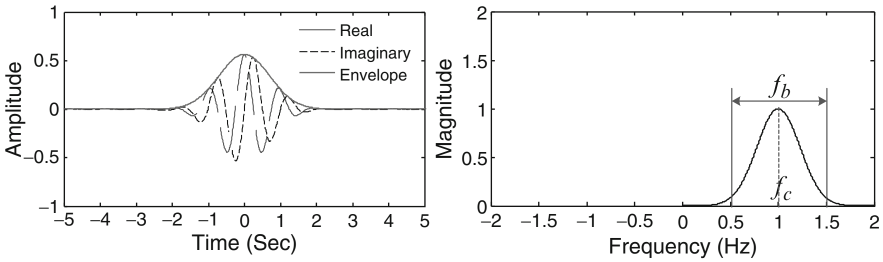

Fig. 3.5 Morlet wavelet (*left*) and its magnitude spectrum (*right*): $f_b = 1$ Hz and $f_c = 1$ Hz

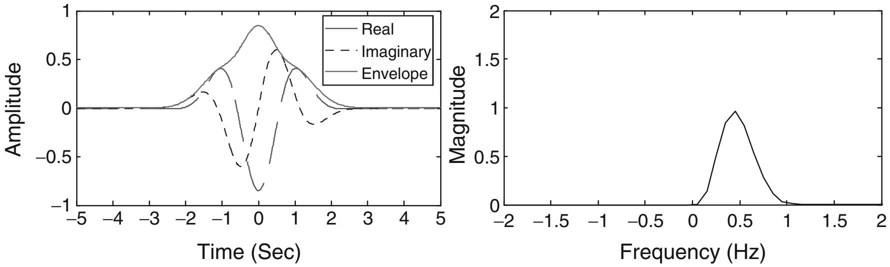

Fig. 3.6 Gaussian wavelet (*left*) and its magnitude spectrum (*right*): $N = 2$

signal, for example, bearing defect-induced vibration (Lin and Qu 2000; Nikolaou and Antoniadis 2002; Yan and Gao 2009).

3.4.3 Gaussian Wavelet

Mathematically, a Gaussian function is expressed as (Teolis 1998)

$$f(t) = e^{-jt} e^{-t^2} \tag{3.31}$$

Taking the Nth derivative of this function yields the Gaussian wavelet as

$$\psi_G(t) = c_N \frac{d^{(N)} f(t)}{dt^N}, \tag{3.32}$$

where N is an integer parameter $(\geqslant 1)$ and denotes the order of the wavelet, and c_N is a constant introduced to ensure that $\|f^{(N)}(t)\|^2 = 1$. Figure 3.6 illustrates the Gaussian function with its magnitude spectrum for the case of $N = 2$. The Gaussian wavelet is often used for characterizing singularity that exists in a signal (Mallat and Hwang 1992; Sun and Tang 2002).

3.4.4 Frequency B-Spline Wavelet

A frequency B-spline wavelet is defined as (Teolis 1998)

$$\psi_{\mathrm{B}}(t) = \sqrt{f_{\mathrm{b}}}\left[\sin\, c\left(\frac{f_{\mathrm{b}}t}{p}\right)\right]^{p} e^{j2\pi f_{\mathrm{c}}t} \tag{3.33}$$

where f_{b} is the bandwidth parameter, f_{c} denotes the wavelet center frequency, and p is an integer parameter $(\geqslant 2)$. The notation of $\sin\, c(\cdot)$ is a $\sin c$ function, which is defined as

$$\sin c(x) = \begin{cases} 1 & x = 0 \\ \frac{\sin x}{x} & \text{otherwise} \end{cases} \tag{3.34}$$

As an example, a B-spline wavelet for the case of $f_{\mathrm{b}} = 1$ Hz, $f_{\mathrm{c}} = 1$ Hz, and $p = 2$ together with its corresponding magnitude function is shown in Fig. 3.7. The application of the frequency B-spline wavelet has been seen in biomedical signal analysis (Moga et al. 2005; Fard et al. 2007).

3.4.5 Shannon Wavelet

The Shannon wavelet is a special case of the frequency B-spline wavelet for $p = 1$:

$$\psi_{\mathrm{S}}(t) = \sqrt{f_{\mathrm{b}}}\sin c(f_{\mathrm{b}}t)\mathrm{e}^{j2\pi f_{\mathrm{c}}t} \tag{3.35}$$

where f_{b} is the bandwidth parameter and f_{c} denotes the wavelet center frequency. The notation of $\sin\, c(\cdot)$ is a $\sin\, c$ function and defined in (3.34). Figure 3.8 illustrates the Shannon wavelet for the case of $f_{\mathrm{b}} = 1$ Hz and $f_{\mathrm{c}} = 1$ Hz, with its corresponding magnitude spectrum. The Shannon wavelet has been shown for the analysis and synthesis of the $1/f$ processes (Shusterman and Feder 1998).

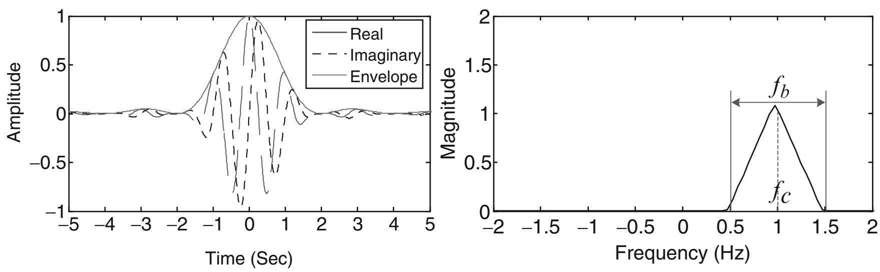

Fig. 3.7 Frequency B-spline wavelet (*left*) and its corresponding magnitude spectrum (*right*): $p = 2, f_{\mathrm{b}} = 1$ Hz, and $f_{\mathrm{c}} = 1$ Hz

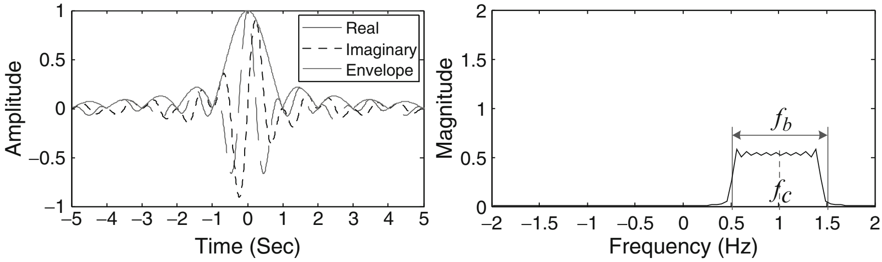

Fig. 3.8 Shannon wavelet (*left*) and its corresponding magnitude spectrum (*right*): $f_b = 1$ Hz and $f_c = 1$ Hz

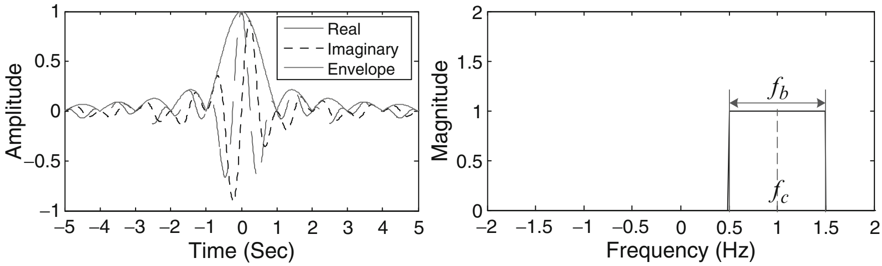

Fig. 3.9 Harmonic wavelet (*left*) and its magnitude spectrum (*right*): $m = 0.5$ Hz and $n = 1.5$ Hz

3.4.6 Harmonic Wavelet

The harmonic wavelet is defined in the frequency domain as (Newland 1994a, b; Yan and Gao 2005)

$$\Psi_{m,n}(f) = \begin{cases} \frac{1}{n-m} & m \leqslant f \leqslant n \\ 0 & \text{elsewhere} \end{cases} \tag{3.36}$$

where the symbols m and n are the scale parameters. These parameters are real but not necessarily integers. Furthermore, the bandwidth f_b and center frequency f_c are determined by the scale parameter as

$$f_b = n - m; \qquad f_c = \frac{n+m}{2} \tag{3.37}$$

As an example, Fig. 3.9 shows the harmonic wavelet function and its corresponding magnitude spectrum for the case of $m = 0.5$ and $n = 1.5$. The harmonic wavelet was first designed by Newland for analyzing vibration signals (Newland 1993). Later, the application of harmonic wavelet has been extended to heart rate variability analysis (Bates et al. 1997) and image denoising (Iftekharuddin 2002).

3.5 CWT of Representative Signals

Using the wavelets introduced in Sect. 3.4, the CWT is applied to several typical signals, as described below.

3.5.1 CWT of Sinusoidal Function

The first signal analyzed is a pure sinusoidal function. Figure 3.10a illustrates a 50 Hz sinusoidal signal, and Fig. 3.10b illustrates the CWT results of the signal. It is seen that the 50 Hz component is present all the time throughout the analysis duration.

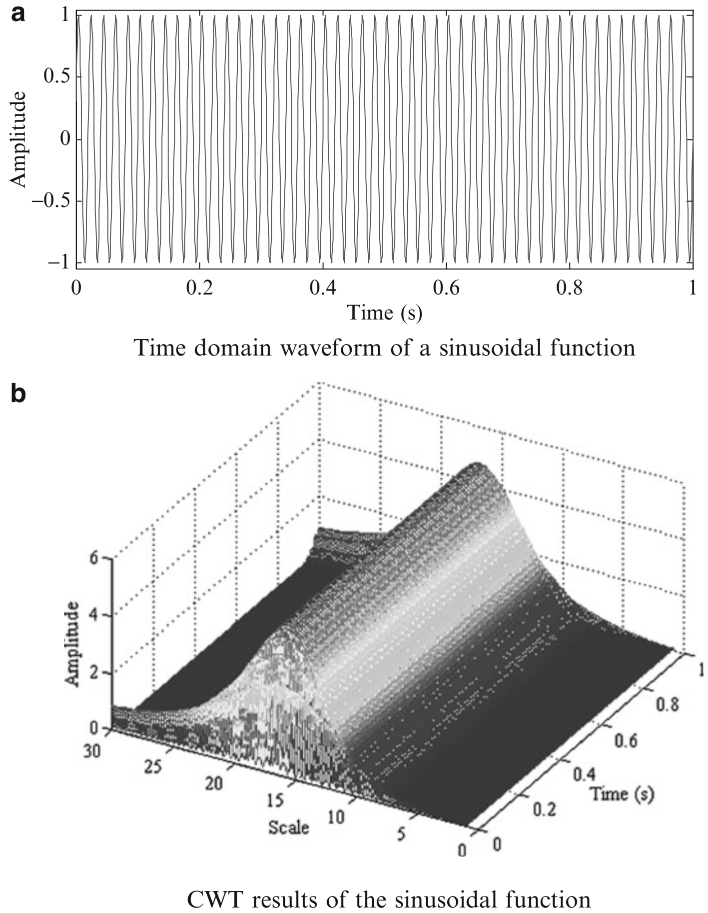

Fig. 3.10 A sinusoidal function (**a**) time domain waveform (**b**) CWT results

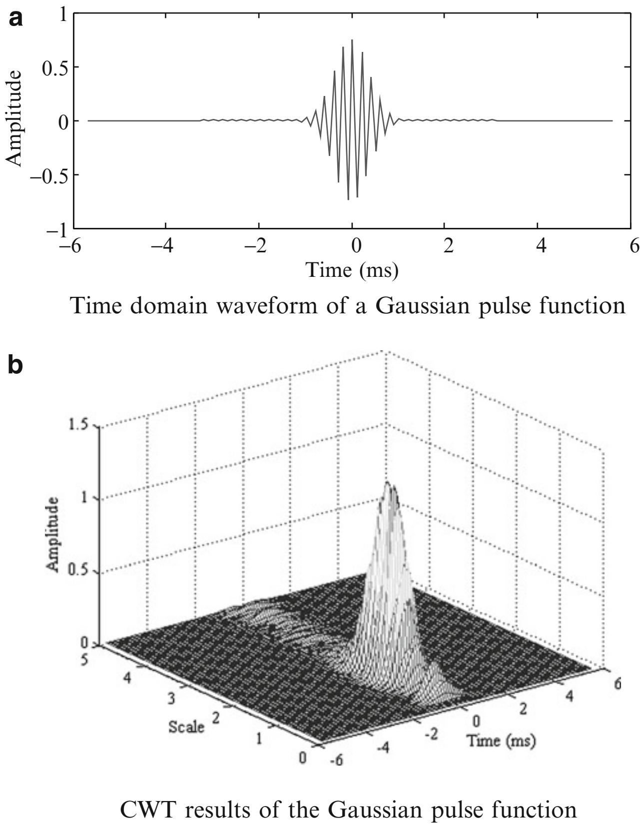

Fig. 3.11 A Gaussian pulse function (**a**) time domain waveform (**b**) CWT results

3.5.2 CWT of Gaussian Pulse Function

The second signal is a Gaussian pulse function. Figure 3.11a shows a Gaussian pulse signal with 10 kHz center frequency. Figure 3.11b illustrates the CWT results of the Gaussian pulse signal, which is identified in the time-scale domain at around 0 s.

3.5.3 CWT of Chirp Function

The last signal is a chirp function. Figure 3.12a shows an example of a chirp signal. It is a linear swept-frequency signal with the instantaneous frequency being 50 Hz at time zero. The instantaneous frequency 10 Hz is achieved after 1 s. Figure 3.12b illustrates the CWT results of the chirp signal, and the change of frequency along with time can be clearly seen.

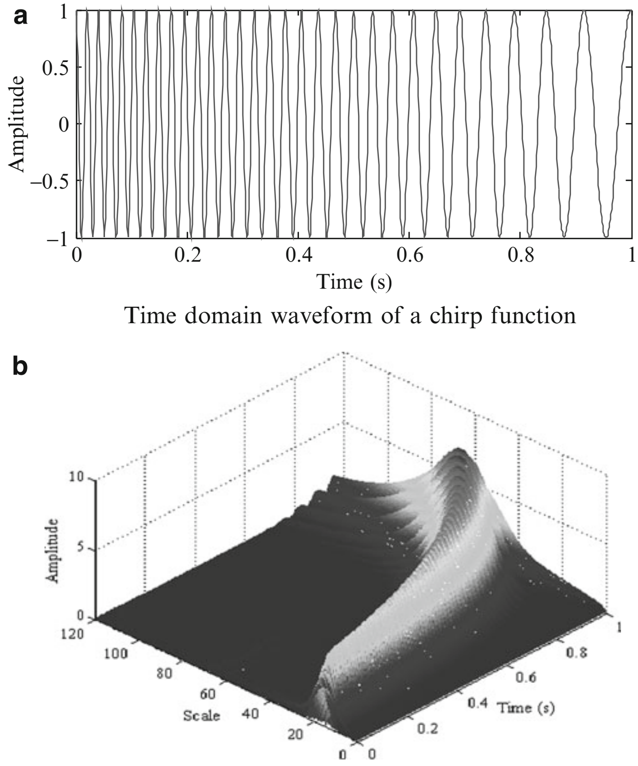

CWT results of the chirp function

Fig. 3.12 A chirp function (**a**) time domain waveform (**b**) CWT results

3.6 Summary

This chapter begins with definition of a wavelet, where the *admissibility condition* that a wavelet should satisfy is emphasized. The CWT and its related properties are then introduced. Two approaches for implementing the CWT are discussed in Sect. 3.3, followed by the introduction of some commonly used wavelets in Sect. 3.4. Typical signals are analyzed using the CWT and the results are shown in Sect. 3.5.

3.7 References

Bates RA, Hilton MF, Godfrey KR, Chappell MJ (1997) Autonomic function assessment using analysis of heart rate variability. Control Eng Pract 5(12):1731–1737

Bracewell R (1999) The Fourier transform and its applications. 3rd edn. McGraw-Hill, New York

Chui CK (1992) An introduction to wavelets. Academic, New York

Daubechies I (1992) Ten lectures on wavelets. SIAM, Philadelphia, PA
Erlebacher G, Yuen DA (2004) A wavelet toolkit for visualization and analysis of large data sets in earthquake research. Pure Appl Geophys 161(11–12):2215–2229
Fard PJ, Moradi MH, Divide MR (2007) A novel approach in R peak detection using hybrid complex wavelet (HCW). Int J Cardiol 124(2):250–253
Grossmann A, Morlet J (1984) Decomposition of hardy functions into square integrable wavelets of constant shape. SIAM J Math Anal 15(4):723–736
Iftekharuddin KM (2002) Harmonic wavelet joint transform correlator: analysis, algorithm, and application to image denoising. Opt Eng 41(12):3307–3315
Lin J, Qu L (2000) Feature extraction based on Morlet wavelet and its application for mechanical fault diagnosis. J Sound Vib 234(1):135–148
Mallat SG (1998) A wavelet tour of signal processing. Academic, San Diego, CA
Mallat SG, Hwang WL (1992) Singularity detection and processing with wavelets. IEEE Trans Inf Theory 38:617–643
Meyer Y (1993) Wavelets, algorithms and applications. SIAM, Philadelphia, PA
Moga M, Moga VD, Mihalas GhI (2005) Continuous wavelet transform in ECG analysis: a concept or clinical uses. Connecting medical informatics and bio-informatics, pp 1143–1148, IOS Press
Newland DE (1993) Random vibrations, spectral and wavelet analysis. Wiley, New York
Newland DE (1994a) Wavelet analysis of vibration part I: theory, ASME J Vib Acoust 116(4):409–416
Newland DE (1994b) Wavelet analysis of vibration part II: wavelet maps, ASME J Vib Acoust 116(4): 417–425
Nikolaou NG, Antoniadis IA (2002) Demodulation of vibration signals generated by defects in rolling element bearings using complex shifted Morlet wavelets. Mech Syst Signal Process 16(4):677–694
Rioul O, Vetterli M (1991) Wavelets and signal processing. IEEE Signal Process Mag 8(4):14–38
Shusterman E, Feder M. (1998) *Analysis and synthesis of 1/f processes via Shannon wavelets. IEEE Trans Signal Process* 46(6):1698–1702
Sun Q, Tang Y (2002) Singularity analysis using continuous wavelet transform for bearing fault diagnosis. Mech Syst Signal Process 16:1025–1041
Teolis A. (1998) Computational signal processing with wavelets. Birkhäuser Boston, MA
Yan R, Gao RX (2005) An efficient approach to machine health diagnosis based on harmonic wavelet packet transform. Robot Comput Integr Manuf 21:291–301
Yan R, Gao R (2009) Multi-scale enveloping spectrogram for vibration analysis in bearing defect diagnosis. Tribol Int 42(2): 293–302
Zhou Z, Adeli H, (2003) Time-frequency signal analysis of earthquake records using Mexican hat wavelets. Comput Aided Civ Infrastruct Eng 18(5):379–389